

XI. RELATIONSHIP BETWEEN LOCAL VARIATION OF NODULE FACIES AND ACOUSTIC STRATIGRAPHY IN THE SOUTHERN PART OF THE CENTRAL PACIFIC BASIN (GH82-4 AREA)

Akira Usui and Manabu Tanahashi

The distribution pattern of regional and local variation of manganese nodules are not necessarily related to topography or water depth. Earlier comparative studies of nodule deposits with acoustic stratigraphy have pointed out some significant evidences of close relationship of nodule abundance or composition to thickness or pattern of substrate sediments (Moore and Heath, 1966; Calvert *et al.*, 1978; Tamaki *et al.*, 1977; Mizuno *et al.*, 1980). Our previous investigations have revealed that thickness of young sediments of Neogene to Quaternary are the most important geological parameter relating to nodule abundance, morphology, and chemistry (Tanahashi, 1977; Usui, 1983; Usui *et al.*, 1987; Usui and Tanahashi, 1987). We made an attempt to find any regularities in variation of nodule facies on the basis of 3.5 kHz sub-bottom profiler (SBP) and air-gun seismic records. The seismic profiles of air gun was less available than SBP for nodule field mapping because of less resolution, even though the uppermost reflectors were generally correlated to each other on both profiles.

According to the previous geological correlations to DSDP cores (Sites 165, 166 and 170) in the northern Central Pacific Basin, substrates of this area are composed of following acoustic units: Unit I (uppermost transparent layer sometimes with internal weak reflectors), Unit II (semi-opaque layer) and acoustic basement (opaque) in the order of age (Tamaki, 1977). Unit I has three variable acoustic features: type A (entirely transparent), type B (generally transparent with concordant reflectors), and type C (generally transparent with flat turbidite beds). He has pointed out that abundant nodules occur with type A which is correlated to the Oligocene to Recent oozes and clays, and that nodule abundance is inversely related to thickness of Unit I of type A.

The GH82-4 area is dominantly covered by Unit I which is classified into three types, although underlain opaque layers may be variable (Tanahashi, chapter IV of this volume). Types B and C are mainly distributed in the western flat basin area, but type A is dominant in the detailed survey area in the eastern part. A general relationship between nodule facies and acoustic stratigraphy was again found in the regional survey area. Western flat basin area where calcareous turbidite beds are frequent within transparent layers yields no nodules (Fig. XI-1). Abundant nodule field is related to the area of type A or the area of absence of Unit I. Nodule type is also variable. Type-r nodules occur together with type A of moderate thickness and

Keywords: transparent layer, acoustic stratigraphy, subbottom profiler, DSDP core, manganese nodule, abundance, Central Pacific Basin, Hakurei-Marui, Nova-Canton Trough

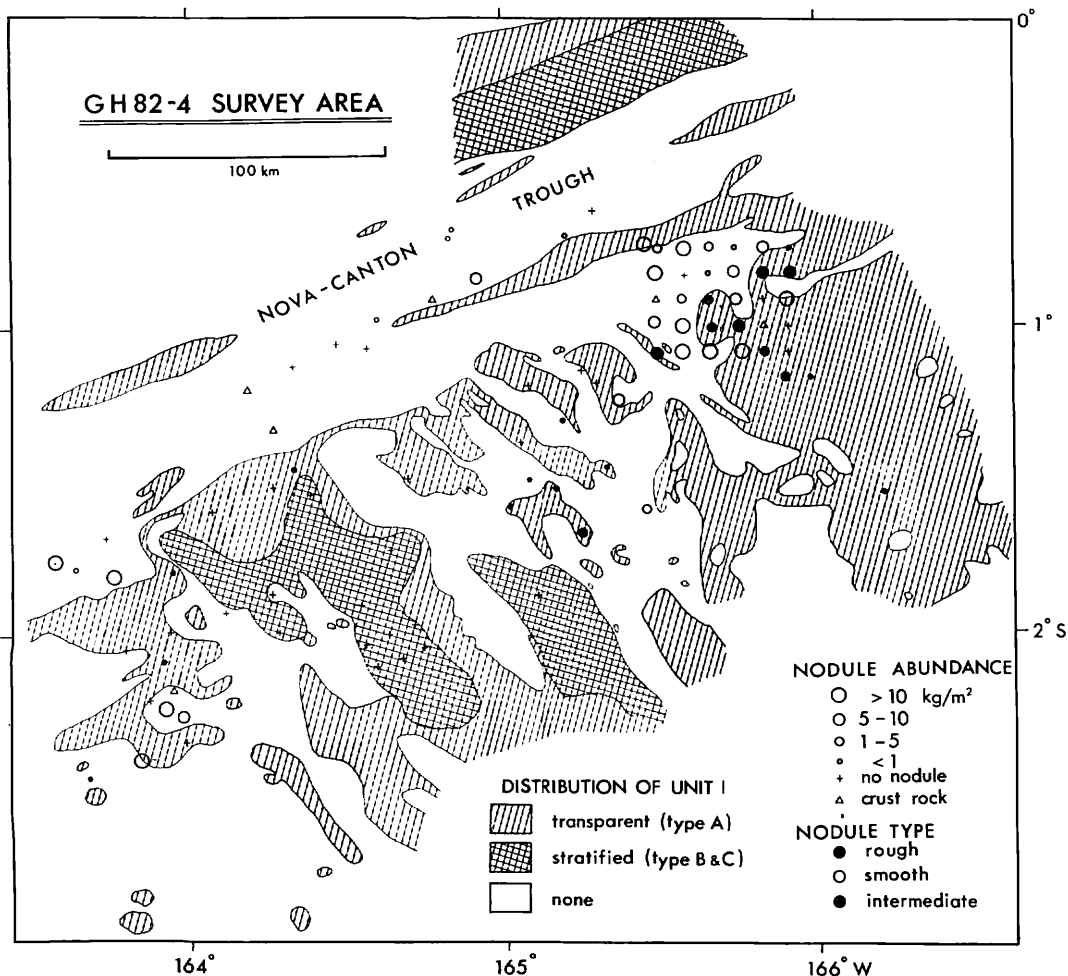


Fig. XI-1 Distribution of manganese nodules and Unit I in the regional survey area.

absence of Unit I is related to type-s nodules.

In the detailed survey area, above-mentioned relationship found during the regional survey is also applicable. The local variation is closely related to the thickness and structure pattern of transparent layers of Unit I. The thickness is variable ranging from zero to more than 100 meters (Table XI-1 and Figure XI-2).

The area of very thick transparent layer (thicker than approximately 80 meters) yields scarce or no nodules, for instance, in the eastern flat basin. Nodules are also barren on the two seamount covered with thick calcareous sediments. The greatest abundance is encountered only in the area of thin transparent layers (60 meters or thinner). However, it seems that the thickness of transparent layers is not always a unique factor controlling nodule abundance, because the abundance is quite variable at a given thickness between 10 to 60 meters (Figs. XI-3 and 4).

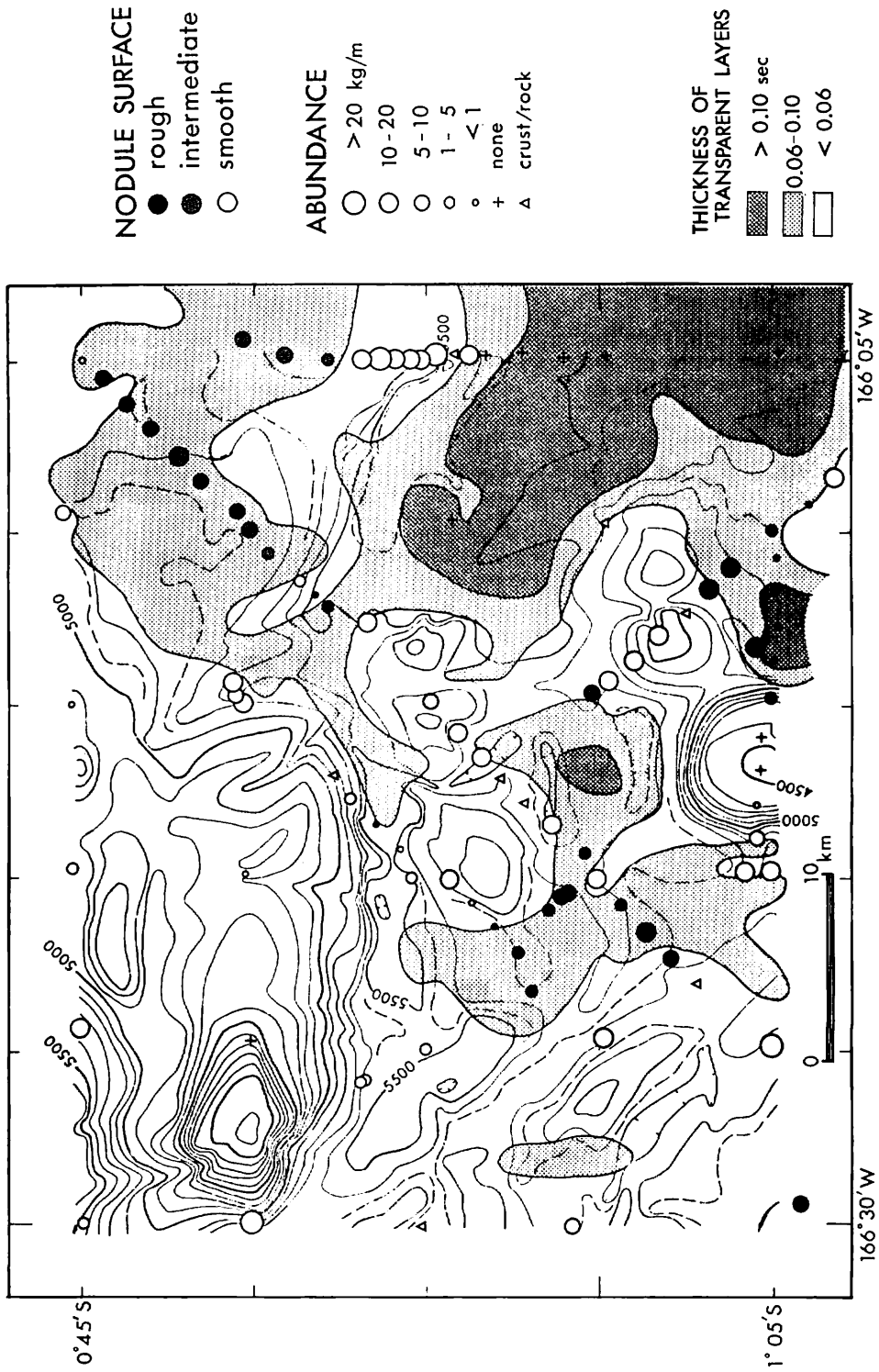


Fig. XI-2 Distribution of manganese nodules and thickness of uppermost transparent layers in the de-tailed survey area. Thickness is shown in two-way travel time in seconds.

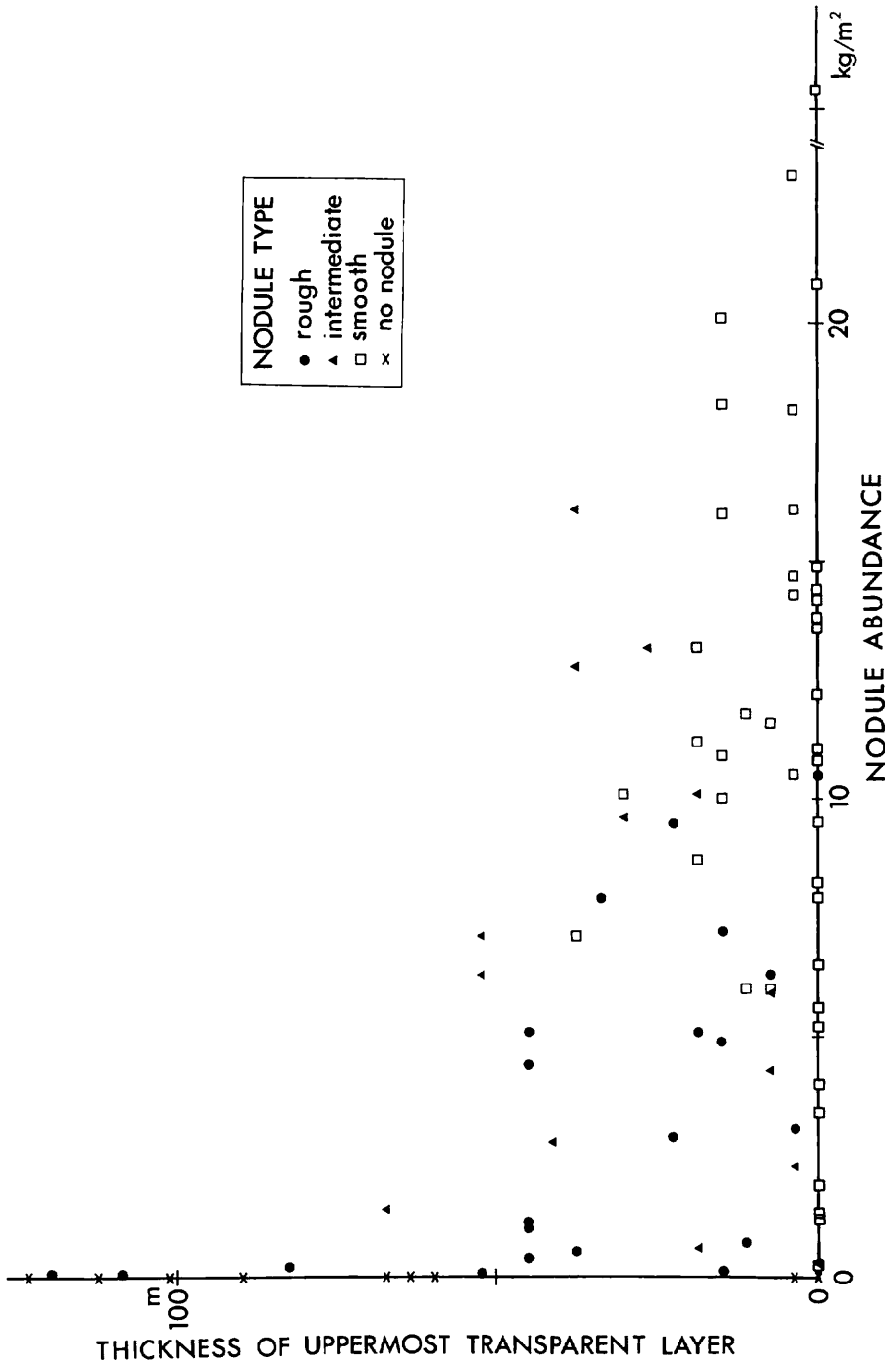


Fig. X1-3 Relationship between nodule abundance and thickness of the uppermost transparent layer (type A of Unit I) on 3.5 kHz SBP records. Sound velocity of sediments is assumed as 1500 m/sec. Data for manganese crusts are not included.

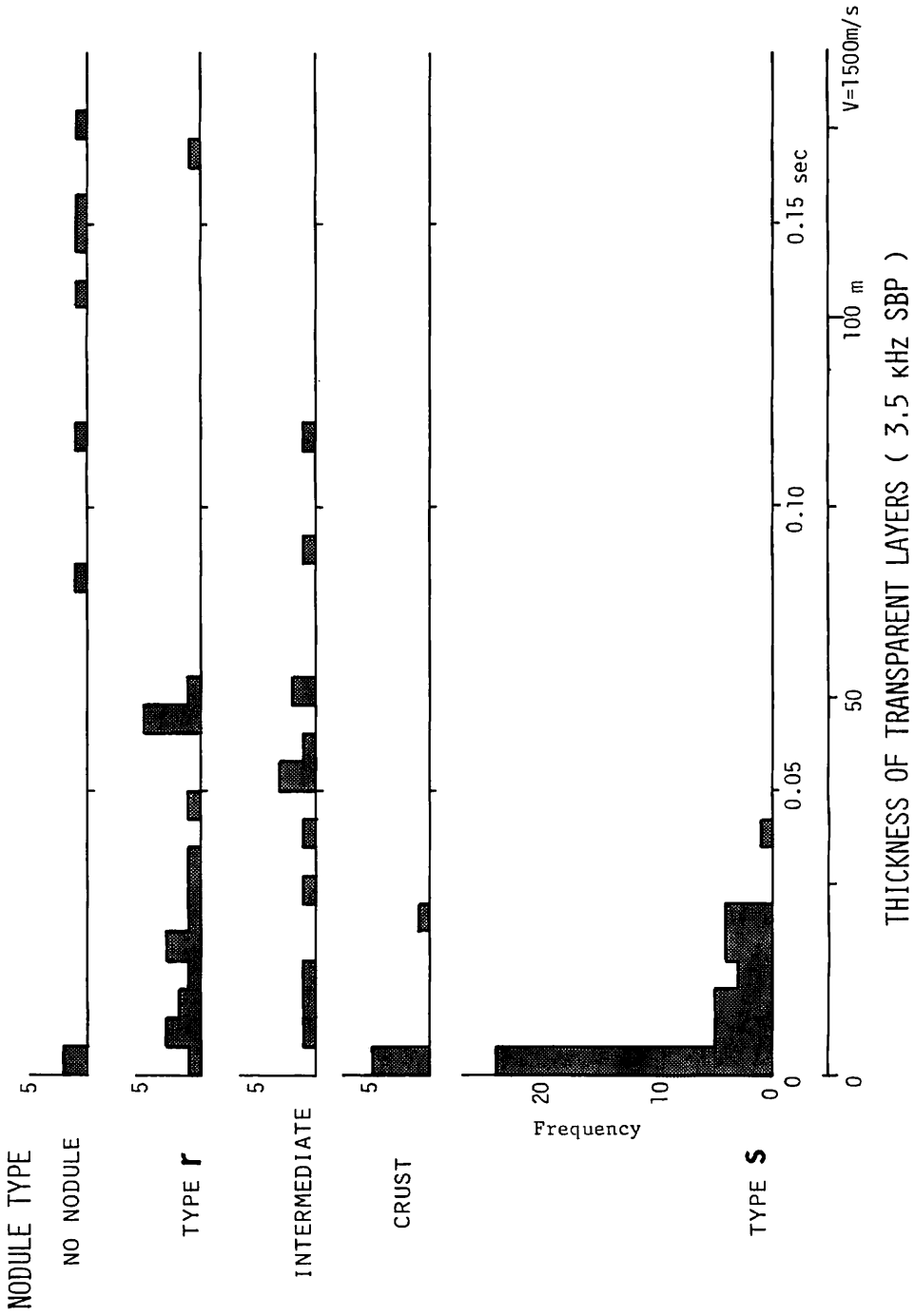


Fig. XI-4 Frequency distribution of thickness of Unit I on 3.5 kHz SBP records and its difference with nodule type.

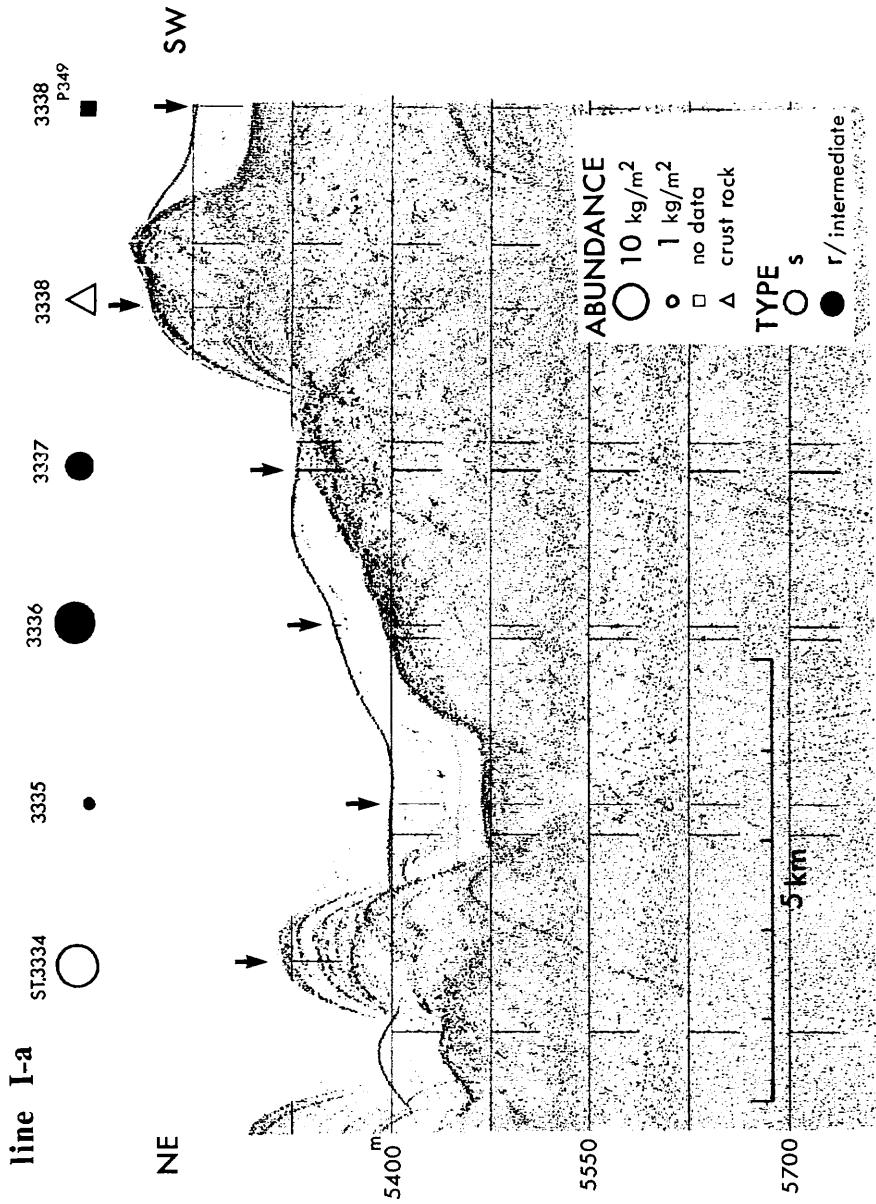


Fig. XI-5 Typical 3.5 kHz SBP profiles and nodule distribution in the detailed survey area. Station numbers, nodule types and abundance are shown for each station (arrows).

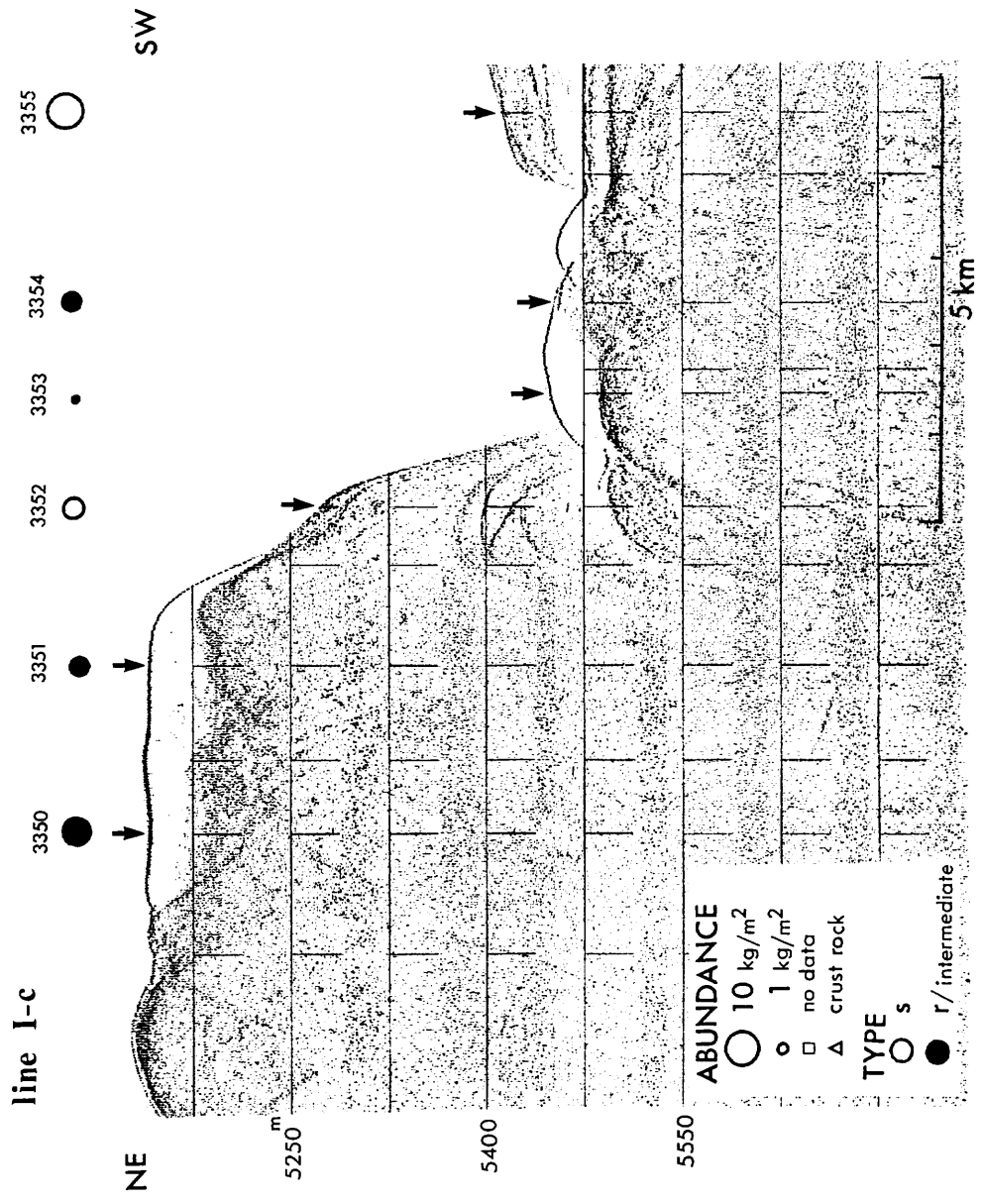


Fig. XI-5 (continued)

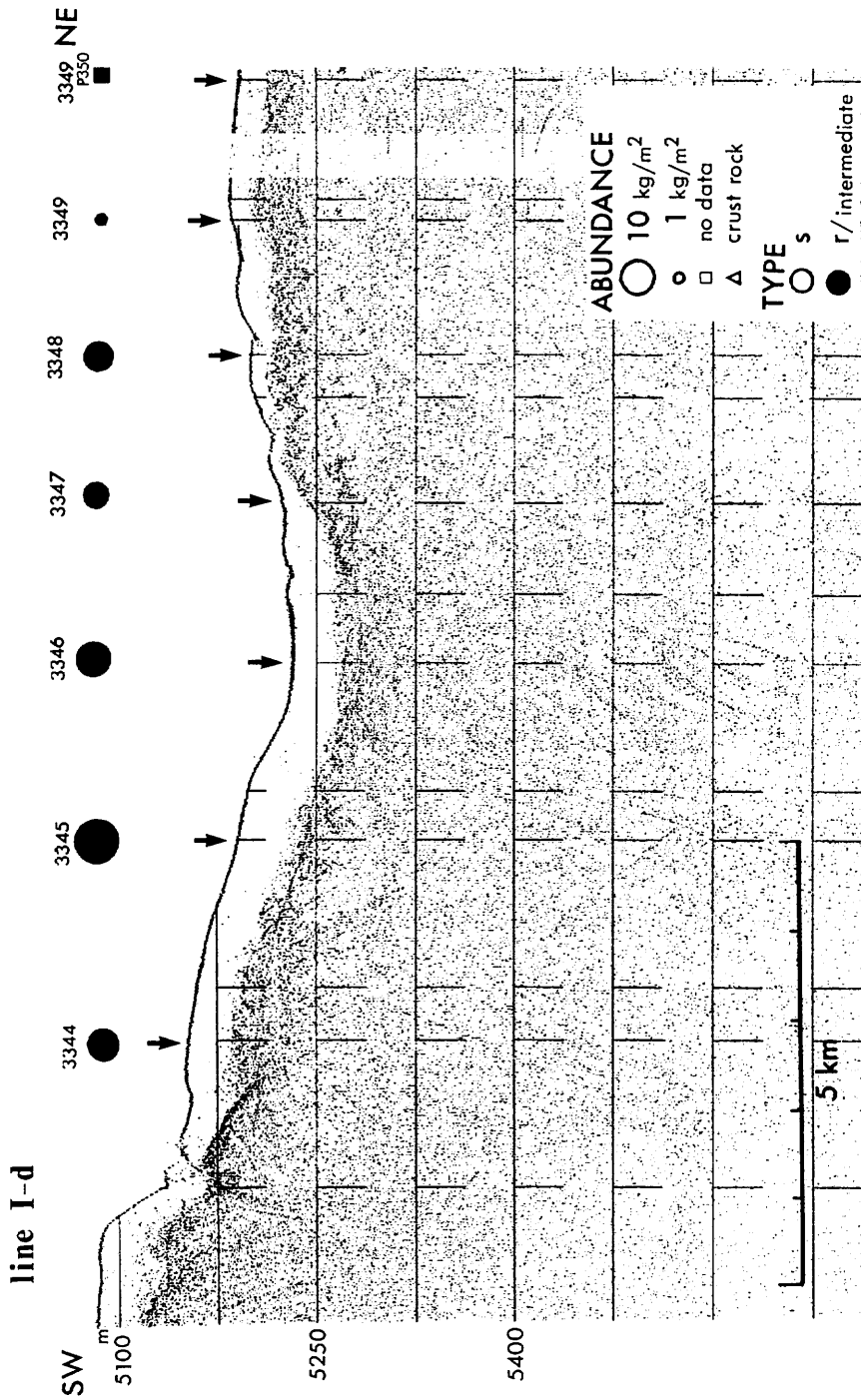


Fig. XI-5 (continued)

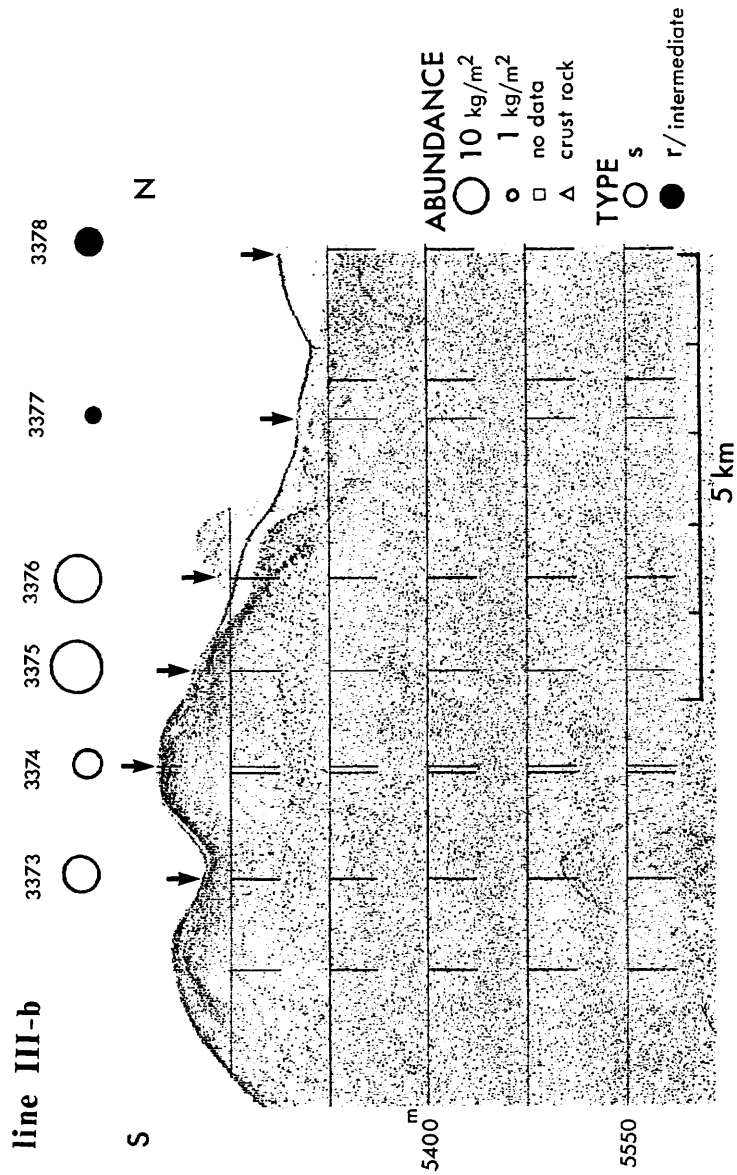


Fig. XI-5 (continued)

Table XI-1 Thickness of Transparent Layer, Nodule Abundance and Morphology.

St./sample no.	Nodule type	bundance (kg/m ²)	Unit l thickness	type							
					3283	FG460	Sr, Vr	tr	60	A	
						B73	Vr	tr	60	A	
3246	FG424	-	0.0	-	3284	FG461	ls.r, Ds.r	9.3	0	A	
3247	FG425	SPs, ISPs, Ts	16.0	15	A	3285	FG462	-	0.0	0	A
3248	FG426-1	IDs, Fs, ls	4.0	0	A	3286	FG463	-	0.0	22	A
	FG426-2	IDs, ls	3.4	0	A	3287	FG464	IDPs, DPs	19.8	0	A
	P336	IDs	-	0	A	3288	FG465	-	0.0	0	B
3249	FG427	DPs	tr	0	A		P340	-	-	0	B
	B70	-	-	0	A	3289	FG466	-	0.0	0	B
3251	FG428	IDs, IDPs, Ts, Fs	5.7	0	A	3290	FG467	-	0.0	18	B
3252	FG429	-	0.0	0	A	3291	FG468	-	0.0	0	B
3253	FG430	Vs	tr	-	-	3292	FG469	-	0.0	0	B
	B71	Vs	tr	-	-	3293	FG470	-	0.0	0	B
3254	FG431	IDs, DPs	0.4	0	A	3294	FG471	-	0.0	0	B
3255	FG432	-	0.0	0	A	3295	FG472	Sr	0.4	45	A
3256	FG433	-	0.0	0	A	3296	FG473	-	0.0	90	A
3257	FG434	-	0.0	0	A	3297	FG474	Sr	2.9	22	A
3258	FG435	IDs, Fs	1.5	0	A	3298	FG475	-	0.0	112	A
3259	FG436	-	0.0	0	A	3299	FG476	Ss.r	7.1	52	A
3260	FG437	Sr?	tr	101	A	3300	FG477	SPs	8.7	18	A
3261	FG438	-	0.0	105	A		B74	SPs	11.2	18	A
3262	FG439	-	0.0	45	A	3301	FG478	(Vr)	tr	108	A
	P337	IDs.r	-	45	A	3302	FG479	-	0.0	18	A
3263	FG440	-	0.0	-	-	3303	FG480	ISs	30.3	0	A
3264	FG441	-	0.0	45	A	3304	FG481	IDs	1.2	0	A
3265	FG442	Sr?	tr	56	A	3305	FG482	-	0.0	0	A
	P338	-	-	60	A	3306	FG483	ISs, IDPs, Fs	11.0	0	A
3266	FG443	-	0.0	90	A	3307	FG484	IDPs, IDs, ISs	1.3	0	A
3267	FG444	IDs, IDPs, Ts, Fs	15.8	0	A	3308	FG485	IDs, Fs	20.1	15	A
3268	FG445	Ds, IDPs, Fs	0.4	0	A	3309	FG486	-	0.0	7	A
3269	FG446	-	0.0	52	B	3310	FG487	IDs, IDPs	6.0	11	A
3270	FG447	-	0.0	0	B	3311	FG488	ISs, IDs	20.8	0	A
3271	FG448	-	0.0	97	B	3312	FG489	IDs, Ds, IDPs	14.7	3	A
	B72	-	0.0	90	B		P341	Ss, SPs	-	-	-
3272	FG449	-	0.0	0	A	3313	FG490	SPs, DPs	9.5	0	A
3273	FG450	-	0.0	90	A	3314	FG491	Ss	0.2	0	A
3274	FG451	(lr)	tr	232	A	3315	FG492	Sr	5.1	45	A
3275	FG452	IDs, Ts, ls	2.3	0	A		P342	-	-	30	A
3276	FG453	lr, Sr	0.1	120	A	3316	FG493	ISs	0.2	0	A
3277	FG454	Sr	3.5	67	A	3317	FG494	Ds.r, DPs.r	4.3	7	A
	P339	-	-	67	A	3318	FG495	IDPs, Ts	8.2	0	A
3278	FG455	Sr	0.1	56	A	3319	D513	Sr	-	-	-
3279	FG456	Sr, lr	tr	26	A	3320	FG496	IDs.r, IDPr	13.2	26	A
3280	FG457	Vr, Sr	tr	33	A	3321	FG497	Sr, SPr	9.5	22	A
3281	FG458	-	0.0	82	A	3322	FG498	Sr	4.4	45	A
3282	FG459	IDs, IDPs	18.6	7	A	3323	FG499	ISPs, IDs	14.2	0	A

Table XI-1 (continued)

3324	B75	IDr, Dr, IDPr, Sr	6.3	7	A	3361	FG528	Sr, Dr	10.5	0	A
	B75X	IDr, IDPr, Dr	-	-	-	3362	FG529	Ss.r, SPs.r	10.1	18	A
3325	P343	-	-	0	B	3363	FG530	-	0.0	0	A
3326	P344	-	-	0	B	3364	FG531	ISs	11.6	7	A
3327	B76	-	0.0	0	B	3365	FG532	IDs, TS, IDPs	10.8	0	A
3328	P345	-	-	60	A	3366	B81	SPs, Ss	10.1	30	A
3329	FG500	-	0.0	67	A	3367	FG533	IDs, IDPs	14.4	0	A
	P346	-	-	67	A	3368	FG534	-	0.0	0	A
3330	B77	-	0.0	60	B	3369	FG535	IDPs, IDs	14.9	0	A
3331	FG501	IDs, IDPs	5.2	0	A	3370	FG536	-	0.0	63	A
	P347	Ss, DPAs	-	30	A	3371	FG537	-	0.0	101	A
3332	FG502	-	0.0	7	A	3372	FG538	-	0.0	123	A
	P348	-	-	7	A		P352	-	-	78	A
3333	B78	Sr	0.1	45	A	3373	FG539	IDs, IDPs	10.5	3	A
3334	FG503	IDs, IDPs	13.6	0	A	3374	FG540	IDs, IDPs	6.5	0	A
3335	FG504	ISs.r, Sr	1.4	67	A	3375	FG541	ISs, IDs	23.1	3	A
3336	FG505	Ss.r, SPs.r	12.8	37	A	3376	FG542	IDs, ISs, IDPs	18.3	15	A
3337	FG506	Ss.r, SPs.r	6.0	7	A	3377	FG543	Is.r, Fs.r	2.3	3	A
3338	FG507	-	0.0	0	A	3378	B82	Ss.r, SPs.r, Ds.r	6.3	52	A
	P349	SPs, ISPs	-	0	A	3379	FG544	ISs, IDs, Fs	6.0	7	A
3339	FG508	IDPs, IDs	18.2	3	A	3380	FG545	Sr	0.1	0	A
3340	FG509	-	-	0	A	3381	FG546	IDs, Fs	1.9	0	A
3341	FG510	IDs	>0.3	0	A	3382	FG547	-	0.0	3	A
3342	FG511	IDs, IDPs	12.6	0	A	3383	FG548	SPs, ISPs	13.2	18	A
3343	B79	IDs, IDPs	16.4	3	A		P353	IDs, IDPs, ISPs	-	11	A
	B79X	IDr+s	12.2	-	A	3384	FG549	IDPs, ISPs, IDs	13.8	0	A
3344	FG512	Sr, SPR	7.9	33	A	3385	FG550	Is	tr	15	A
3345	FG513	Ss.r	16.1	37	A	3386	FG551	Sr	tr	52	A
3346	FG514	Ss.r, SPs.r	9.6	30	A	3387	FG552	Sr, Dr	1.1	45	A
3347	FG515	Sr	5.1	18	A	3388	B83	Sr	1.0	45	A
3348	FG516	Sr	7.2	15	A	3389	FG553	(Tr, Vr)	1.1	45	A
3349	FG517	SPs.r, ISs.r	0.6	18	A	3390	FG554	Sr	0.7	11	A
	P350	Ss.r	-	18	A	3391	FG555	(Vr)	tr	120	A
3350	FG518	SPs, Ss, ISPs	.1	37	A	3392	FG556	Vr, Sr	0.2	82	A
3351	FG519	Ss.r	2.8	41	A	3393	FG557	Sr, Vr, Fr	0.1	15	A
3352	FG520	IDPs, IDs, ISPs	4.0	0	A	3394	P354	-	-	-	-
3353	FG521	Sr, Dr, Vr	0.5	37	A	3395	FG558	-	0.0	3	A
3354	FG522	Sr, Dr	3.1	3	A	3396	FG559	-	0.0	0	A
3355	B80	IDPs, ISPs, IDs	10.9	15	A	3397	FG560	Fs.r, Sr	0.3	0	A
	B80X	ISs, IDs	10.9	-	-	3398	FG561	ISs, IDs, Fs	5.6	0	A
3356	FG523	(Sr)	tr	0	A	3399	B84	IDPs, IDs	11.8	11	A
3357	FG524	Ts, IDs, Ts+r	14.3	3	A		B84X	IDPs, IDs	>3.8	-	-
3358	FG525	Ts, IDs	4.0	-	-	3400	P355	IDs	-	0	A
3359	FG526	IDs, Ts, Ts+r	10.0	15	A	3401	C19	-	-	-	-
3360	FG527	Sr, Dr	4.9	15	A	3402	FG562	ISs, IDs	1.2	0	A
	P351	-	-	15	A	3403	D514	SPs.r, Ss.r	-	-	-

Another important rule on nodule facies and acoustic stratigraphy in detailed survey areas is that nodule type is clearly related to the development of Unit I (Fig. XI-3). Nodules of type s are preferentially distributed in the area of scarce or no development of Unit I. Apparent outcrops of older opaque layers are related to abundant distribution of type-s nodules or manganese crust, while moderate development of transparent layers is to type r (Fig. XI-5). In contrast, r-type nodules are related to moderate development of Unit I with variable abundance. Along line I-c, for instance, type-r nodules are dominant in the northern flat elevated area and smooth surface nodules are very locally distributed in a very narrow area of apparent outcrop of opaque layers (Fig. XI-5).

These relationships found in the GH82-4 area is generally similar to those found in the GH81-4 and GH79-1 areas, regionally in the northern Central Pacific Basin (Mizuno *et al.*, 1980) and on the Wake-Tahiti Transect (Usui, 1982). The relationship is consistent with the two supply route model for nodule formation; type s is composed of hydrogenetic components derived from normal sea water in an oxidizing condition and type r is composed of diagenetic components derived from unconsolidated surface biogenous sediment (Usui, 1979; Halbach and Özkara, 1979). No or scarce sedimentation appear to be a requisite for an abundant deposition of s-type nodules, while a moderate sedimentation of siliceous sediments for development of r-type nodules (Fig. XI-4).

The relationships have been probably controlled by Antarctic Bottom Waters, productivity of organic materials, and movement of the Pacific plate. A great variation of nodule type in this area may be due to distance from high productivity zone. As this area is located in the margin of equatorial high-productivity zone, diagenetic process is influenced by slight change of local sedimentary conditions. Detailed correlations of nodule variabilities to sediment stratigraphy should be discussed at each site, on the basis of nodule and sediment chronological data.

References

- Calvert, S. E., Price, N. B., Heath, G. R. and Moore, T. C. (1978) Relationship between ferromanganese nodule compositions and sedimentation in a small survey area of the equatorial Pacific. *J. Mar. Res.*, vol. 36, p. 161-183.
- Halbach, P. and Ozkara, M. (1979) Morphological and geochemical classification of deep-sea ferromanganese nodules and its genetic interpretation. In: C. Lalou (ed.), *La Genèse des Nodules de Manganèse. C. N. R. S. Rept.*, no. 289, p. 77-88.
- Mizuno, A., Miyazaki, T., Nishimura, A., Tamaki, K. and Tanahashi, M. (1980) Central Pacific manganese nodules, and their relation to sedimentary history. *Proc. Offshore Technology Conference in Houston, May 5-8, 1980*, (OTC3830), p. 331-340.
- Moore, T. C. Jr. and Heath G. R. (1966) Manganese nodules, topography, and thickness of Quaternary sediments in the Central Pacific. *Nature*, 212, p. 983-985.
- Tamaki, K. (1977) Study on substrate stratigraphy and structure by continuous seismic

- reflection profiling survey. In: A. Mizuno and T. Moritani (eds.), *Geol. Surv. Japan Cruise Rept.*, no. 8, p. 51-62.
- , Honza, E. and Mizuno, A. (1977) Relation between manganese nodule distribution and acoustic stratigraphy in the eastern half of the Central Pacific Basin. In: Mizuno, A. and Nakao, S. (eds.), *Geol. Surv. Japan Cruise Rept.*, no. 8, p. 172-176.
- Tanahahi, M. (1977) The uppermost transparent layers and manganese nodule deposits in the Central Pacific Basin. *Marine Science (monthly)*, vol. 15, no. 7, p. 432-436, in Japanese.
- Usui, A. (1979) Minerals, metal contents and mechanism of formation of manganese nodules from the Central Pacific Basin (GH76-1 and GH77-1 areas). In: Bischoff, J. L. and Piper, D. Z. (eds.), *Marine Geology and Oceanography of the Pacific Manganese Nodule Province*, Plenum, New York, pp. 651-677.
- (1982) Variability of manganese nodule deposits: the Wake-Tahiti Transect. In: Mizuno, A. and Nakao, S. (eds.), *Geol. Surv. Japan Cruise Rept.*, no. 18, p. 138-223.
- (1983) Regional variation of manganese nodule facies on the Wake-Tahiti Transect: morphological, chemical and mineralogical study. *Mar. Geol.*, vol. 54, p. 27-51.
- , Nishimura, A., Tanahashi, M. and Terashima, S. (1987) Local variability of manganese nodule facies on small abyssal hills of the Central Pacific Basin. *Mar. Geol.*, vol. 74, p. 237-275.
- and Tanahashi, M. (1987) Relationship between local variation of manganese nodule facies and acoustic stratigraphy in the GH81-4 area. In: Nakao, S and Moritani, T. (eds.), *Geol. Surv. Japan Cruise Rept.*, no. 21, p. 160-170.